AMERICAN SOCIETY FOR MICROBIOLOGY | Antimicrobial Agents and Chemotherapy®

MECHANISMS OF RESISTANCE

Defining Substrate Specificity in the CTX-M Family: the Role of Asp240 in Ceftazidime Hydrolysis

Barbara Ghiglione,[a,b] María Margarita Rodríguez,[a,b] Lucrecia Curto,[b,d] Florencia Brunetti,[a] Milena Dropa,[c] Robert A. Bonomo,[e,f,g] Pablo Power,[a,b] Gabriel Gutkind[a,b]

[a]Universidad de Buenos Aires, Facultad de Farmacia y Bioquímica, Departamento de Microbiología, Inmunología y Biotecnología, Laboratorio de Resistencia Bacteriana, Buenos Aires, Argentina

[b]Consejo Nacional de Investigaciones Científicas y Técnicas (CONICET), Buenos Aires, Argentina

[c]Faculdade de Saúde Pública, Universidade de São Paulo, São Paulo, Brazil

[d]IQUIFIB, Universidad de Buenos Aires, Facultad de Farmacia y Bioquímica, Buenos Aires, Argentina

[e]Medical Service and GRECC, Louis Stokes Cleveland Department of Veterans Affairs Medical Center, Cleveland, Ohio, USA

[f]Departments of Medicine, Pharmacology, Molecular Biology and Microbiology, Biochemistry, Proteomics and Bioinformatics, Case Western Reserve University School of Medicine, Cleveland, Ohio, USA

[g]CWRU-Cleveland VAMC Center for Antimicrobial Resistance and Epidemiology (Case VA CARES), Cleveland, Ohio, USA

ABSTRACT The natural diversification of CTX-M β-lactamases led to the emergence of Asp240Gly variants in the clinic that confer reduced susceptibility to ceftazidime (CAZ). In this study, we compared the impact of this substitution on CAZ and ceftazidime-avibactam (CZA) MICs against isogenic *Escherichia coli* strains with different porin deficiencies. Our results show a noticeable increase in CAZ resistance in clones expressing Asp240Gly-harboring CTX-M when combined with OmpF porin deficiency. Kinetic analysis revealed that the k_{cat}/K_m for CAZ was 5- to 15-fold higher for all Asp240Gly variants but remained 200- to 725-fold lower than that for cefotaxime (CTX). *In vitro* selection of CAZ-resistant clones yielded nonsusceptible CTX-M producers (MIC of >16 μg/ml) only after overnight incubation; the addition of avibactam (AVI) decreased MICs to a susceptible range against these variants. In contrast, the use of CZA as a selective agent did not yield resistant clones. AVI inactivated both CTX-M-12 and CTX-M-96, with an apparent inhibition constant comparable to that of SHV-2 and 1,000-fold greater than that of PER-2 and CMY-2, and k_2/K for CTX-M-12 was 24- and 35-fold higher than that for CTX-M-96 and CTX-M-15, respectively. Molecular modeling suggests that AVI interacts similarly with CTX-M-96 and CTX-M-15. We conclude that the impact of Asp240Gly in resistance may arise when other mechanisms are also present (i.e., OmpF deficiency). Additionally, CAZ selection could favor the emergence of CAZ-resistant subpopulations. These results define the role of Asp240 and the impact of the -Gly substitution and allow us to hypothesize that the use of CZA is an effective preventive strategy to delay the development of resistance in this family of extended-spectrum β-lactamases.

KEYWORDS Asp240Gly, CTX-M-96, OmpF, avibactam, cefotaxime, ceftazidimase, ceftazidime, ceftazidime-avibactam

To date, CTX-M β-lactamases represent the most prevalent group of extended-spectrum β-lactamases (ESBLs) among pathogens around the world, representing a global pandemic (1–3). Since their initial identification, more than 180 allelic variants have been described (ftp://ftp.ncbi.nlm.nih.gov/pathogen/betalactamases/Allele.tab). Each variant can be categorized into at least five genetically distinct groups or clusters. Each cluster includes CTX-M variants with less than 5% amino acid sequence differences

Received 18 January 2018 **Returned for modification** 7 February 2018 **Accepted** 5 April 2018

Accepted manuscript posted online 9 April 2018

Citation Ghiglione B, Rodríguez MM, Curto L, Brunetti F, Dropa M, Bonomo RA, Power P, Gutkind G. 2018. Defining substrate specificity in the CTX-M family: the role of Asp240 in ceftazidime hydrolysis. Antimicrob Agents Chemother 62:e00116-18. https://doi.org/10.1128/AAC.00116-18.

Address correspondence to Pablo Power, ppower@ffyb.uba.ar.

within each group. Notably, a considerable number of CTX-M β-lactamases are encoded by the chromosome of *Kluyvera* species, a microorganism commonly found in the environment and sporadically isolated from clinical settings, where the CTX-M β-lactamases have been apparently recruited as native ESBL genes by recombination and mobilization events and have subsequently disseminated into a variety of pathogens (2, 4, 5).

Microorganisms producing acquired CTX-M β-lactamases are generally resistant to most β-lactams, including penicillins, narrow-spectrum cephalosporins, and the oxyiminocephalosporins cefotaxime (CTX) and ceftriaxone. MICs for ceftazidime (CAZ), carbapenems, and 7-α-methoxy-cephalosporins such as cefoxitin usually remain in the susceptible range. Like other class A serine-β-lactamases, CTX-M β-lactamases are inhibited by first-generation mechanism-based β-lactamase inhibitors (clavulanate, sulbactam, and tazobactam) (6, 7). Avibactam (AVI), a novel non-β-lactam β-lactamase inhibitor that has been recently approved for therapeutic use in combination with CAZ, also inhibits CTX-M β-lactamases (8), as well as the boronic acid pharmacophore derivative vaborbactam (9).

Several amino acids are identified as functionally important for the ESBL activity of CTX-M β-lactamases; among them, amino acids in the structurally flexible β3-strand and the Ω-loop and residues such as Asn104, Ser237, Asp240, and Arg276, which are located in the vicinity of the active site, appear to be involved in the preferred cefotaxime-hydrolyzing activity of CTX-M enzymes (10). Several investigations revealed that their hydrolytic activity is determined not only by substrate recognition and catalysis but also by the maintenance of their conformational integrity and stability due to the contribution of residues distal to the active site (11). Also, certain combinations of amino acid residues may be responsible for the presence of more variants belonging to a specific cluster and their higher capacity of expanding their substrate profile (12). A proper understanding of the contribution of each residue to catalysis has implications for the future design of novel cephalosporin antibiotics and for antibiotic stewardship.

Compared to other ESBLs, CTX-M β-lactamases hydrolyze CTX more efficiently than CAZ. Previous investigations by Delmas et al. indicated that binding of CTX in CTX-M-9 β-lactamase results in a conformational change in the active site, involving disruption of a hydrogen bond between main-chain groups of Asn170 and Asp240 that connects the Ω-loop to the β3 strand. The result of this change is the expansion of the active site to allow adequate positioning of CTX for catalysis, which was hypothesized to contribute to the "cefotaximase" activity of the CTX-M enzymes (13). The crystal structures of the CTX-M-14 variants Ser70Gly, Ser70Gly:Ser237Ala, and Ser70Gly:Ser237Ala:Arg276Ala, both in the apo form and in complex with CTX, revealed the importance of residues Ser237 and Arg276 in establishing the interactions with CTX and their cooperativity in shaping the active site in the region of Asn170 and Asp240 via indirect bridging interactions through the CTX molecule (14).

Diversification of CTX-M β-lactamases has led to the emergence of Asp240Gly and Pro167Ser variants that broaden the substrate profile and confer on the producing microorganisms decreased susceptibility to CAZ (2, 6). The Asp240Gly substitution is the most prevalent (15–17), resulting in an up to 8-fold increase in CAZ MIC values in the harboring microorganisms (18–20). The improved hydrolytic efficiency of Asp240Gly mutants toward CAZ appears to be associated with a higher flexibility of β3, although this substitution is also correlated with lower stability (15). Moreover, it should be noted that Asp240Gly substitutions are selected more frequently than amino acid changes at Pro167, probably because modifications in residues comprising the Ω-loop result in a larger active site that allows accommodation of CAZ for hydrolysis but also a significant decrease in stability (21, 22).

To understand the impact of Gly instead of an Asp at position 240, we compared the activity of representatives from each of the five main phylogenetic groups of CTX-M against the oxyimino-cephalosporins CTX and CAZ. Additionally, we explored the effect of these substitutions in combination with porin deficiencies in an isogenic *Escherichia*

coli background. Our goal is to understand and anticipate if these changes are associated with high-level CAZ-resistant variants, alone or combined with AVI.

RESULTS AND DISCUSSION

CTX-M variants containing the Asp240Gly substitution confer remarkable resistance to CAZ only in isogenic strains lacking OmpF. In this work, we analyzed the susceptibility profile of one representative variant of all five phylogenetic clusters within the CTX-M family to detect differences that may be the consequence of functionally important amino acid substitutions among each group that could influence the hydrolytic activity. Expression of CTX-M β-lactamases in an isogenic *E. coli* DH5α background allowed us to directly evaluate and compare the activities of β-lactams and β-lactam–β-lactamase inhibitor combinations (23).

All *E. coli* DH5α recombinant clones expressing CTX-M β-lactamases exhibited a resistance profile compatible with the presence of these enzymes (Table 1), that is, a differential behavior that yields high-level resistance to CTX but spares CAZ or confers only reduced susceptibility to the latter. As expected, addition of clavulanic acid decreased MICs of CTX and CAZ, rendering isolates susceptible to the combination.

MICs of CTX and CAZ against *E. coli* K-12-derived strains are shown in Table 2. Using Clinical and Laboratory Standards Institute (CLSI) breakpoints as a reference, all clones demonstrated resistance to CTX. We detected a noticeable increase in CAZ resistance only in those *E. coli* K-12 strains expressing CTX-M variants containing Asp240Gly when combined with OmpF porin deficiency. In previous investigations, we demonstrated that an alteration in OmpC expression yields intermediate resistance to CAZ (24). Therefore, alterations in OmpF porin expression or any other mechanism leading to a diminished amount of CAZ availability in the periplasm for blocking the target penicillin-binding proteins seems to be an important determinant for achieving resistance levels similar to those observed in clinical isolates producing a CTX-M β-lactamase harboring the Asp240Gly substitution.

All Asp240Gly CTX-M variants displayed slight increases in activity toward CAZ. An efficiency factor (EF) can be defined as the ratio between the catalytic efficiencies of CTX-M^{Gly240} and CTX-M^{Asp240} toward a specific β-lactam. For CAZ, the k_{cat}/K_m was between 5- and 15-fold higher for all CTX-M^{Gly} variants, with CTX and CEF having the highest values among the substrates compared. Nevertheless, even when CTX-M^{Gly} variants displayed a higher increase in the catalytic efficiency toward CAZ than CTX-M^{Asp}, it remained between 200- and 725-fold lower than that for CTX (Table 3).

Using competition assays between CAZ and nitrocefin, we did not observe perceptible inhibition of any CTX-M variant, even after using up to 5 mM CAZ, confirming that K_m for this antibiotic reached values in the millimolar range (data not shown). Also, upon preincubation of the enzyme with increasing concentrations of CAZ, a slight inhibition was observed only after at least 2 h of preincubation. These results suggest that efficient hydrolysis of CAZ could only occur with either high concentrations of CAZ in the medium and/or after prolonged incubation times with the enzyme, two conditions that do not mimic *in vivo* treatment.

The hydrolytic efficiencies toward CEF and CTX were consistently higher for CTX-M-8^{Asp240Gly} and CTX-M-78^{Asp240Gly} variants than for their respective wild-type CTX-M, suggesting that polymorphisms in clusters 8 and 25 play a special role in modulating the expression of this substitution (22). We also observed that gaining some activity toward CAZ did not represent a loss of hydrolytic efficiency toward CEF or CTX. In fact, the Asp240Gly mutation does not seem to have a deleterious impact on the overall resistance phenotype of *E. coli* strains producing CTX-M Asp240Gly variants, as summarized in Table 1; all CTX-M producers remained resistant to penicillins as well as narrow- and expanded-spectrum cephalosporins, and only the MIC of CAZ increased by two or more dilutions in all Asp240Gly variants except CTX-M-131.

We previously demonstrated that CTX-M-96 was efficiently inhibited by both clavulanic acid and tazobactam, with the sulfone as a more potent inhibitor (24). As for

TABLE 1 MICs of *E. coli* DH5α recombinant clones

Antibiotic	MIC (μg/ml) for *E. coli* DH5α harboring:											
	Wild tpe	pK19	pK12 (CTX-M-12)	pK96 (CTX-M-96	pK2 (CTX-M-2)	pK131 (CTX-M-131)	pK8 (CTX-M-8)	pK8^{Asp240Gly} (CTX-M-8^{Asp240Gly})	pK9 (CTX-M-9)	pK16 (CTX-M-16)	pK78 (CTX-M-78)	pK78^{Asp240Gly} (CTX-M-78^{Asp240Gly})
Ampicillin	1	1	>256	>256	>256	>256	>256	>256	>256	>256	>256	>256
Piperacillin	2	2	>256	>256	>256	>256	>256	>256	>256	>256	>256	>256
Cephalothin	4	4	>512	>512	>512	>512	>512	>512	>512	>512	>512	>512
Cefotaxime	≤0.125	≤0.125	>128	>128	>128	>128	>128	>128	>128	>128	>128	>128
Cefotaxime + clavulanic acid	≤0.125	≤0.125	≤0.125	≤0.125	≤0.125	≤0.125	≤0.125	≤0.125	≤0.125	≤0.125	≤0.125	≤0.125
Ceftazidime	≤0.125	≤0.125	1	32	2	1	2	8	1	8	1	16
Ceftazidime + clavulanic acid	≤0.125	≤0.125	≤0.125	≤0.125	≤0.125	≤0.125	≤0.125	≤0.125	≤0.125	≤0.125	≤0.125	≤0.125
Cefepime	≤0.125	≤0.125	8	2	16	32	1	2	2	2	4	2
Cefoxitin	2	2	4	4	1	0.5	4	4	2	4	4	2
Imipenem	≤0.5	≤0.5	≤0.5	≤0.5	≤0.5	≤0.5	≤0.5	≤0.5	≤0.5	≤0.5	≤0.5	≤0.5

TABLE 2 MICs of oxyiminocephalosporins for *E. coli* K-12 and derived isogenic porin-deficient strain JF703 (OmpF$^-$) expressing CTX-M from the corresponding pK19-derived constructions

CTX-M group[a]	MIC[b] (μg/ml) of:							
	Cefotaxime				CAZ			
	Asp240		Gly240		Asp240		Gly240	
	K-12	JF703	K-12	JF703	K-12	JF703	K-12	JF703
1	128	256	128	128	4	8	8	32
2	256	256	256	256	16	8	8	32
8	256	64	256	256	4	4	16	64
9	256	128	128	128	1	4	8	32
25	256	256	256	256	0.25	2	8	32

[a]Group 1, CTX-M-12 (Asp240) and CTX-M-96 (Gly240); group 2, CTX-M-2 (Asp240) and CTX-M-131 (Gly240); group 8, CTX-M-8 (Asp240) and CTX-M-8mut (Gly240); group 9, CTX-M-9 (Asp240) and CTX-M-16 (Gly240); group 25, CTX-M-78 (Asp240) and CTX-M-78mut (Gly240).
[b]MIC of CTX and CAZ, respectively, for control strains: *E. coli* K-12 (<0.25 and <0.5), *E. coli* K-12/pK19 (<0.25 and <0.5), *E. coli* JF703 (0.25 and <0.5), *E. coli* JF703/pK19 (0.25 and <0.5), and *E. coli* ATCC 25922 (0.25 and <0.5).

CEF and CTX, it seemed that Asp240Gly mutation did not impair the ability of clavulanic acid to block the β-lactamases due to the susceptibility profile of all clones tested, where the MIC for CAZ/CLA was $\leq$0.125 μg/ml.

The Asp240Gly substitution neither affects the overall conformation nor alters thermal stability. A biophysical characterization was carried out for evaluating the impact of amino acid substitutions on CTX-M enzyme conformation and stability. Circular dichroism (CD) spectra (Fig. 1A and B) indicate secondary structure preservation (Fig. 1A), while minimal perturbations in tertiary structure are noted (Fig. 1B). In this regard, hardly any structural changes are observed among CTX-Ms containing either Asp or Gly in position 240. Despite their observed similarity in the overall inferred

TABLE 3 Comparative steady-state kinetic parameters of CTX-M β-lactamases

Group and β-lactamase[b]	Cephalothin			Cefotaxime			Ceftazidime[a]		
	k_{cat} (s^{-1})	K_m (μM)	k_{cat}/K_m ($\mu M^{-1} \cdot s^{-1}$)	k_{cat} (s^{-1})	K_m (μM)	k_{cat}/K_m ($\mu M^{-1} \cdot s^{-1}$)	k_{cat} (s^{-1})	K_m (μM)	k_{cat}/K_m ($\mu M^{-1} \cdot s^{-1}$)
1									
CTX-M-12	973 ± 68	130 ± 5	7.5 ± 0.8	78 ± 4	44 ± 3	1.8 ± 0.2	ND	ND	(6 ± 0.06) × 10^{-4}
CTX-M-96	120 ± 4	27 ± 3	4.5 ± 0.7	60 ± 2	34 ± 2	1.7 ± 0.2	ND	ND	(3 ± 0.03) × 10^{-3}
EF			0.6			0.9			5
2									
CTX-M-2	518 ± 30	98 ± 5	5.3 ± 0.6	23 ± 1	19 ± 2	1.2 ± 0.2	ND	ND	(4 ± 0.04) × 10^{-4}
CTX-M-131	142 ± 6	23 ± 3	6.0 ± 0.9	93 ± 4	70 ± 3	1.3 ± 0.2	ND	ND	(6 ± 0.06) × 10^{-3}
EF			1.1			1.1			15
8									
CTX-M-8	306 ± 31	164 ± 10	1.9 ± 0.3	12 ± 0.2	14 ± 1	0.9 ± 0.1	ND	ND	(4 ± 0.04) × 10^{-4}
CTX-M-8^{Asp240Gly}	229 ± 7	78 ± 3	3.0 ± 0.2	21 ± 0.2	7 ± 1	2.9 ± 0.3	ND	ND	(4 ± 0.2) × 10^{-3}
EF			1.6			3.2			10
9									
CTX-M-9	705 ± 28	188 ± 4	3.8 ± 0.2	42 ± 3	42 ± 4	1.0 ± 0.1	ND	ND	(2 ± 0.02) × 10^{-4}
CTX-M-16	220 ± 4	35 ± 2	6.4 ± 0.6	68 ± 3	45 ± 2	1.5 ± 0.1	ND	ND	(3 ± 0.06) × 10^{-3}
EF			1.7			1.5			15
25									
CTX-M-78	289 ± 23	193 ± 10	1.5 ± 0.2	14 ± 1	27 ± 3	0.5 ± 0.1	ND	ND	(3 ± 0.06) × 10^{-4}
CTX-M-78^{Asp240Gly}	37 ± 1	13 ± 5	2.8 ± 1.0	12 ± 0.2	8 ± 1	1.4 ± 0.2	ND	ND	(3 ± 0.09) × 10^{-3}
EF			1.9			2.8			10

[a]ND, not determined by direct hydrolysis.
[b]Efficiency factor (EF) is the ratio between k_{cat}/K_M of Gly240 mutant and Asp240 wild-type β-lactamases.

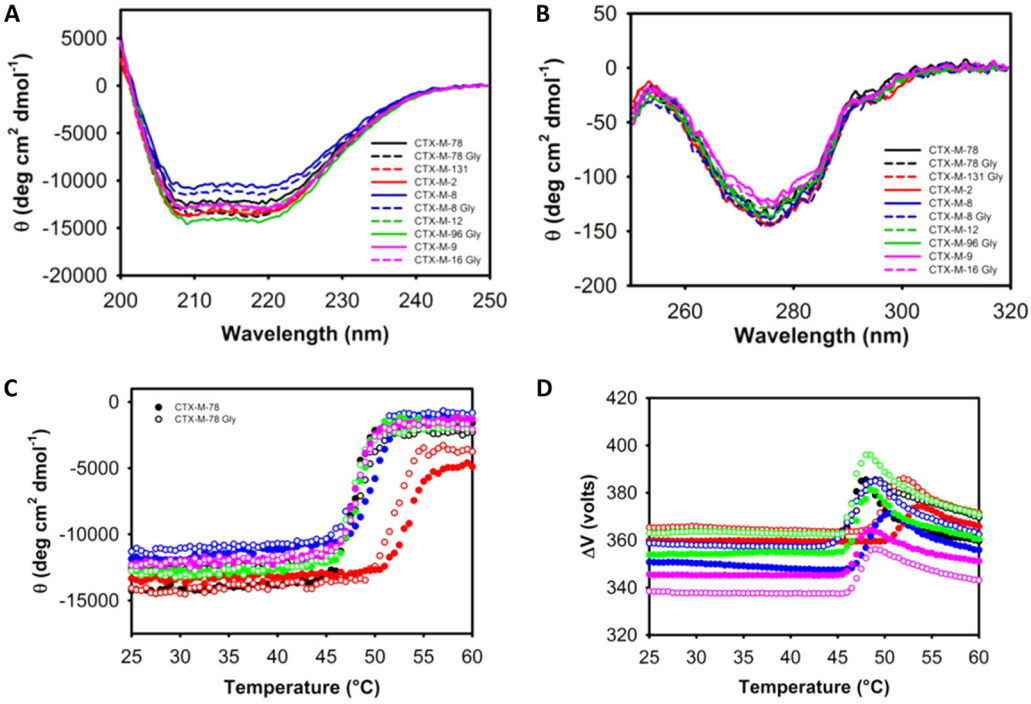

FIG 1 (A and B) Far-UV (A) and near-UV (B) CD spectra for CTX-M^{Asp} (solid line) and CTX-M^{Gly} (dashed line) variants. (C and D) Thermally induced unfolding transitions. CD measurements were recorded for CTX-M^{Asp} (closed symbols) and CTX-M^{Gly} (open symbols) as temperature increased. (C) The transitions were monitored by the evolution of the molar ellipticity at 222 nm. (D) The value of the dynode voltage under each condition is shown.

structure, CD spectra of the 5 representative phylogenetic groups of CTX-M are almost indistinguishable, although local rearrangements cannot be ruled out.

To understand the global impact of the substitution on the stability of these proteins, we proceeded to evaluate their temperature denaturation profiles (Fig. 1C). The evolution of the dynode voltage can be recorded simultaneously along with the collection of CD data (Fig. 1D). An increase in its value reveals the presence of turbidity due to the appearance of protein aggregates, allowing a direct correlation between protein conformational changes and an aggregation behavior (25). For all CTX-M variants, both processes occur concomitantly, revealing that the transitions are inherently irreversible and cannot be analyzed by a formalism assuming thermodynamic equilibrium. In such cases, the temperature of the onset of aggregation (*To*) was obtained. Briefly, this value is derived after fitting a straight line to the initial time points and extrapolating backwards to intersect the temperature abscissa (26).

As judged for the almost invariant *To* value, for the pairs CTX-M-12/CTX-M-96, CTX-M-9/CTX-M-16, and CTX-M-78^{Asp}/CTX-M-78^{Gly}, we did not observe stability differences between proteins carrying Asp or Gly (45.8/45.6, 45.9/46.2, and 45.0/45.4°C, respectively). Indeed, these 3 protein groups have remarkably similar stability. On the other hand, CTX-M-8 and CTX-M-2 show a somewhat higher stability (47.0 and 50.5°C, respectively). For both proteins, the Asp240Gly substitution leads to a 2°C reduction in their *To* values.

CZA combination prevents the *in vitro* selection of CAZ-resistant strains. *In vitro* selection of CAZ-resistant *E. coli* clones yielded CTX-M-96 (CTX-M-12 with Asp240Gly mutation) producers with MIC values of 32 and 64 μg/ml. Notably, CTX-M-12-producing clone variants were obtained even at 16 μg/ml, the resistance breakpoint according to the CLSI (Fig. 2). Our data also demonstrated that CAZ MICs can increase quickly, especially under selective pressure. The nature of the variants selected was not further investigated in this work, but the presence of the Asp240Gly substitution and resistance conferred might contribute to the emergence of porin-deficient strains responsible for

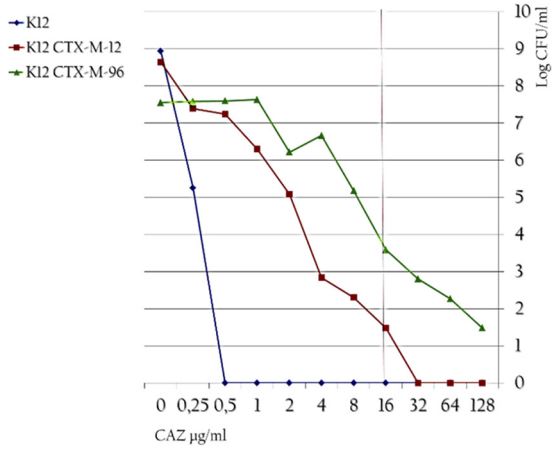

FIG 2 Population analysis profile of *E. coli* K-12 strains expressing CTX-M-12 and CTX-M-96 recovered under CAZ pressure selection.

infections in patients being treated with this antibiotic, as observed in this study for the OmpF-deficient strains, although other mechanisms should not be discarded. However, adaptation also could have been reached by acquisition of mutations enhancing transcription of $bla_{\text{CTX-M}}$ genes, affecting efflux properties, or by selective drift of a clonal population with better fitness under CAZ pressure, which may explain the selection of CTX-M-12-producing clones even at 16 μg/ml (27).

The addition of AVI decreased the MICs of the *E. coli* K-12-derived strains and the two mutants selected in the population analysis (Table 4). More interestingly, the use of the CZA combination as a selective agent yielded only one colony at 1 μg/ml CAZ and 4 μg/ml AVI for *E. coli* K-12 expressing CTX-M-12 and 0.25 μg/ml CAZ and 4 μg/ml AVI μg/ml for CTX-M-96.

Inhibitory effect of AVI against CTX-M variants. The inhibitory effect of AVI observed above is supported by the inhibition constants obtained for both CTX-M-12 and CTX-M-96. The apparent inhibition constant ($K_{i\ \text{app}}$), determined by plotting $1/v_0$ versus AVI concentration, was 4 $\pm$ 0.6 nM for CTX-M-12 and 98 $\pm$ 10 nM for CTX-M-96. These values are comparable to constants derived for studying SHV-2 (28) and up to 1,000 lower for PER-2 and CMY-2 (29, 30).

On the other hand, acylation and encounter complex binding for AVI occur with a k_2/K value of (4.8 $\pm$ 0.3) $\times$ 10^6 M^{-1} s^{-1} and (2.0 $\pm$ 0.1) $\times$ 10^5 M^{-1} s^{-1} for CTX-M-12 and CTX-M-96, respectively. The acylation efficiency for other class A β-lactamases range from 2.2 $\times$ 10^3 M^{-1} s^{-1} in the case of PER-2 (30) to 10^5 M^{-1} s^{-1} for TEM-1 and CTX-M-15 (31, 32).

It is worth nothing that CTX-M-12, which possesses an Asp at 240, displayed a k_2/K value 24-fold higher than that of CTX-M-96 (and ~35-fold that for CTX-M-15), harboring

TABLE 4 CAZ and CAZ-AVI (4 μg/ml) MIC for mutant *E. coli* K-12 clones expressing CTX-M-96

Strain	MIC (μg/ml)	
	CAZ	CZA
E. coli K-12	≤0.25	≤0.25
E. coli JF703	0.25	≤0.25
E. coli K-12/pK12	4	≤0.25
E. coli K-12/pK96	8	0.25
E. coli JF703/pK12	8	0.25
E. coli JF703/pK96	32	≤0.25
E. coli K-12-MUT1[a]	32	0.25
E. coli K-12-MUT2[a]	64	≤0.25

[a]Mutants selected *in vitro* (see the text for details).

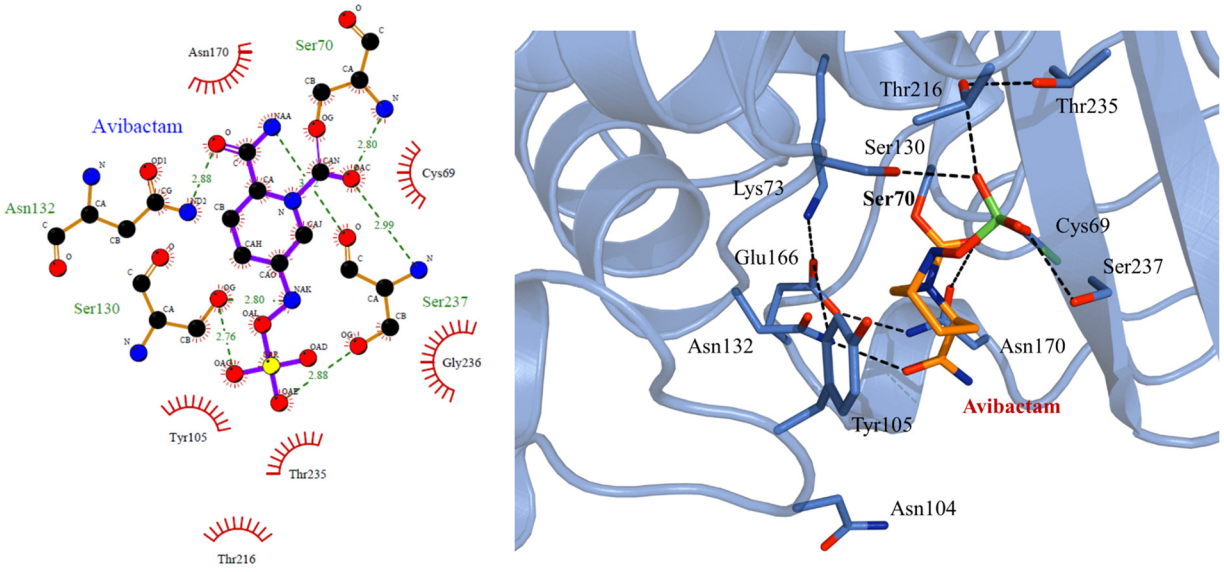

FIG 3 (Left) Two-dimensional representation of CTX-M-96 (Gly240) in association with AVI (created with LigPlot+); green dotted lines represent hydrogen bonds (HB), and red semicircles denote putative hydrophobic interactions. (Right) Three-dimensional *in silico* modeling showing the detailed interaction between AVI and CTX-M-96 residues; black dotted lines represent favored HB (see the text for further discussion).

the Asp240Gly substitution. This is accompanied by $K_{i\ app}$ values 24-fold more favorable for CTX-M-12 and suggest that, even when AVI inhibits CTX-M enzymes, the presence of a glycine residue slightly reduces the acylation efficiency at the expense of some hydrogen bond loss (see below).

CTX-M-96/AVI and CTX-M-15/AVI complexes reveal similar features. To correlate the observed phenotypic and kinetic behavior of AVI in the inhibition of CTX-M and support its efficacy in protecting against the *in vivo* selection of CAZ-resistant clones, simulated models of the β-lactamase in association with AVI were obtained using the coordinates of the CTX-M-96 crystallographic structure.

By analyzing the model of CTX-M-96 with AVI (Fig. 3), we hypothesize that AVI interacts similarly with both CTX-M-96 and CTX-M-15, showing overall equivalent interaction patterns through favored hydrogen bonds. For both enzymes, the six-membered ring of AVI was observed in a chair conformation, interacting with the protein through three key interactions, i.e., (i) the covalent bond that forms the acyl-enzyme complex and interactions with both the (ii) sulfate and (iii) carboxamide groups. AVI appears to be stabilized by hydrogen bonds with residues Ser70, Ser130, Asn132, and Ser237, with the C-7 carbonyl group of the open AVI molecule well positioned in the oxyanion hole. As observed in CTX-M-15, Ser237 may also interact with both the sulfate group and the carboxamide ends of the AVI molecule. Also, the AVI molecule adjusts in the active site in a way in which the deacylating water, observed in other CTX-M-AVI complexes, could efficiently enable the turnover (Fig. 3).

According to our model, hydrophobic interactions are expected to occur between AVI and residues Cys69, Tyr105, Asn170, Thr216, Thr235, and Gly236. In particular, hydrophobic stacking between AVI's piperidine group and Tyr105 side chain seems to be well conserved among the class A β-lactamases (33, 34).

Conclusions. The global spread of CTX-M β-lactamases has led to a significant increase in the use of carbapenems, with the resulting emergence of carbapenemase-producing *Enterobacteriaceae*. Based on available clinical trial data and animal experiments, the CLSI maintains that the MIC is a better predictor of an antibiotic's therapeutic efficacy than defining the underlying resistance mechanism. In this regard, an infection produced by a microorganism susceptible to CAZ can be treated with this antibiotic even if a CTX-M enzyme is present (27); the caveat here is that the MIC is within the susceptible range. This led us to evaluate the activity of CAZ against an

isogenic panel of *E. coli* strains expressing five representative pairs of Asp240/Gly240 CTX-Ms and selecting one of those pairs for evaluating the effect of OmpF deficiency on CAZ susceptibility and the ability of CAZ alone or combined with AVI for *in vivo* selection of resistant clones.

Our results show that CTX-M Asp240Gly expression does not always result in a resistance phenotype; high-level resistance can occur only after ancillary resistance mechanisms are present (lack of OmpF in our case). More relevant to our studies, subpopulations resistant to CAZ are present under nonselective conditions, even in clones expressing wild-type CTX-M under subinhibitory MIC values that may be selected under monotherapy treatment with this antibiotic. Also, as the inoculum effect strongly influences the MIC of CAZ, therapeutic failure in cases of CTX-M-producing (CAZ-susceptible) bacteria is always a possibility, especially in critically ill patients with serious infections such as intra-abdominal abscesses, where a heavy inoculum of bacteria may be present (35).

Nevertheless, the use of cephalosporins for ESBL treatment could result in a lower selective pressure against drugs such as the carbapenems. Most CTX-M are still inhibited by first-generation β-lactamase inhibitors, like clavulanic acid, sulbactam, and tazobactam, although recently two new CTX-M Asp240Gly, Ser130Thr variants that are highly resistant to tazobactam and sulbactam, but not to clavulanic acid, have emerged (36–38).

We stress that the evolution of CTX-M enzymes along the Asp240 pathway appears to be favored in the simultaneous presence of both CTX and CAZ selective pressure (39). This could be explained in part because the Asp240Gly substitution neither affects the overall conformation nor drastically reduces thermal stability, in contrast to Pro167Ser substitution in CTX-M-14 (21). As previously stated, novel β-lactamase inhibitors (BLI) are needed for providing protection to some of the most valuable antibiotics in clinical practice (40, 41). A possible preventive strategy is to delay the development of both cephalosporin and BLI resistance using certain combinations, i.e., the use of AVI (42). More relevant, confirming the presence of a certain resistance mechanism (ESBL and/or AmpC, for instance) and not only MIC determination may still be of value in selecting a targeted antibiotic therapy, as previously suggested (43).

MATERIALS AND METHODS

Bacterial strains and plasmids. Genes encoding $bla_{\text{CTX-M-12}}$, $bla_{\text{CTX-M-96}}$ ($bla_{\text{CTX-M-12}}$ with natural mutation Asp240Gly), $bla_{\text{CTX-M-2}}$, $bla_{\text{CTX-M-8}}$, $bla_{\text{CTX-M-9}}$, and $bla_{\text{CTX-M-78}}$ were amplified from previously characterized clinical isolates stored in our laboratory. *Escherichia coli* ATCC 25922 was used for quality control in antimicrobial susceptibility assays (44). *E. coli* DH5α (Invitrogen, USA) and *E. coli* BL21(DE3) (Novagen, USA) were hosts for transformation experiments. *E. coli* K-12 and its derived isogenic strain, *E. coli* JF703 (lacking *ompF*), were used for assessing the influence of porin deficiency in the overall resistance profile (45). These strains were obtained from the *E. coli* Genetic Stock Center (CGSC; Yale University). Plasmid vectors pTZ57R/T (InsTAclone PCR cloning kit; Thermo Scientific, USA) and pK19 were used for routine cloning experiments (46), while kanamycin-resistant pET28a(+) (Novagen, Germany) was used as the expression vector.

Chemical compounds. CAZ, cefotaxime (CTX), and cephalothin (CEF) were obtained from Klonal (Argentina). Avibactam (AVI) was acquired through an investigator-initiated trial with Actavis (now Allergan). Nitrocefin (NCF) was purchased from Becton-Dickinson and Oxoid.

Recombinant DNA methodology. The $bla_{\text{CTX-M-12}}$, $bla_{\text{CTX-M-96}}$ ($bla_{\text{CTX-M-12}}$ with Asp240Gly mutation), $bla_{\text{CTX-M-2}}$, $bla_{\text{CTX-M-8}}$, $bla_{\text{CTX-M-9}}$, and $bla_{\text{CTX-M-78}}$ genes were amplified by PCR from whole DNA belonging to the corresponding clinical strains using the cloning primers listed in Table 5. Genes for CTX-M with Asp240Gly mutation, $bla_{\text{CTX-M-131}}$ ($bla_{\text{CTX-M-2}}$ with Asp240Gly mutation), $bla_{\text{CTX-M-8}}$ with Asp240Gly mutation, $bla_{\text{CTX-M-16}}$ ($bla_{\text{CTX-M-9}}$ with Asp240Gly mutation), and $bla_{\text{CTX-M-78}}$ with Asp240Gly mutation were generated by site-directed mutagenesis using $bla_{\text{CTX-M}}$ genes with Asp in position 240 as templates. In brief, combinations of mutagenic and cloning primers (Table 1) were used to generate two partially overlapping DNA fragments. These fragments were subsequently used in an overlap extension reaction to amplify the entire coding sequence with the cloning primers. All PCRs were performed using Phusion high-fidelity DNA polymerase (Thermo Scientific, Tecnolab, Argentina) and 1 μM primers. PCR products were cloned at the SmaI site of pK19 vector and transformed in competent *E. coli* DH5α, yielding recombinant plasmids pK12, pK96, pK2, pK131, pK8, pK8Asp240Gly, pK9, pK16, pK78, and pK78Asp240Gly. For overexpression, these plasmids were used as templates for PCRs using Thermo Scientific Phusion high-fidelity DNA polymerase (Thermo Scientific, Tecnolab, Argentina) and 1 μM expression primers listed in Table 1, containing restriction sites that allowed the oriented cloning of the mature β-lactamase's coding sequence. The PCR products were first ligated in a pTZ57R/T vector and the

TABLE 5 Primers used for cloning, expression, and site-directed mutagenesis

Primer	Sequence (5′-3′)[a]	Use
CTX-M-Group1 FpK	AAATGGTTAAAAAATCACTGC	Cloning in pK19 of CTX-M-12 and CTX-M-96
CTX-M-Group1 RpK	CTACAAACCGTCGGTGACGAT	Cloning in pK19 of CTX-M-12 and CTX-M-96
CTX-M-Group2 FpK	TAATGATGACTCAGAGCATTCGC	Cloning in pK19 of CTX-M-2 and CTX-M-131
CTX-M-Group2 RpK	GCATCAGAAACCGTGGGTTACG	Cloning in pK19 of CTX-M-2 and CTX-M-131
CTX-M-2 Asp240Gly Fw	GCAGCGGAGGTTATGGCAC	Site-directed mutagenesis
CTX-M-2 Asp240Gly Rv	GTGCCATAACCTCCGCTGC	Site-directed mutagenesis
CTX-M-Group8 FpK	AGATGATGAGACATCGCGTTAAGC	Cloning in pK19 of CTX-M-8 and CTX-M-8^{Asp240Gly}
CTX-M-Group8 RpK	TTAATAACCGTCGGTGACG	Cloning in pK19 of CTX-M-8 and CTX-M-8^{Asp240Gly}
CTX-M-8 Asp240Gly Fw	CAGCGGTGGTTATGGTACGACG	Site-directed mutagenesis
CTX-M-8 Asp240Gly Rv	CGTCGTACCATAACCACCGCTG	Site-directed mutagenesis
CTX-M-Group9 FpK	AGATGGTGACAAAGAGAGTGC	Cloning in pK19 of CTX-M-9 and CTX-M-16
CTX-M-Group9 RpK	TTACAGCCCTTCGGCGATG	Cloning in pK19 of CTX-M-9 and CTX-M-16
CTX-M-9 Asp240Gly Fw	GGCGGCTACGGCACCACCAATG	Site-directed mutagenesis
CTX-M-9 Asp240Gly Rv	CATTGGTGGTGCCGTAGCCGCC	Site-directed mutagenesis
CTX-M-78 FpK	GGATGATGAGAAAAAGCGTAAGGC	Cloning in pK19 of CTX-M-78 and CTX-M-78^{Asp240Gly}
CTX-M-78 RpK	GGACTAATAACCGTCGGTGAC	Cloning in pK19 of CTX-M-78 and CTX-M-78^{Asp240Gly}
CTX-M-78 Asp240Gly Fw	GCGGCGGTTATGGTACGACGAATG	Site-directed mutagenesis
CTX-M-78 Asp240Gly Rv	CATTCGTCGTACCATAACCGCCGC	Site-directed mutagenesis
PFNdeG1ht	CTGCATATGCAAACGGCGGACG	Expression in pET28a of CTX-M-12 and CTX-M-96
PRHindG1ht	AAGCTTACAAACCGTCGGTGACG	Expression in pET28a of CTX-M-12 and CTX-M-96
PFNheG2ht	GCTAGCCAGGCGAACAGCGTGCAA	Expression in pET28a of CTX-M-2 and CTX-M-131
PREcoG2ht	GAATTCTCAGAAACCGTGGGTT	Expression in pET28a of CTX-M-2 and CTX-M-131
PFNheG8/25ht	CTGTATGCTAGCGCGAACGA	Expression in pET28a of CTX-M-8 and CTX-M-8^{Asp240Gly} Expression in pET28a of CTX-M-78 and CTX-M-78^{Asp240Gly}
PRHindG8/25ht	AAGCTTAATAACCGTCGGTG	Expression in pET28a of CTX-M-8 and CTX-M-8^{Asp240Gly} Expression in pET28a of CTX-M-78 and CTX-M-78^{Asp240Gly}
PFNdeG9ht	CTTCATATGCAGACGAGTGCGG	Expression in pET28a of CTX-M-9 and CTX-M-16
PRHindG9ht	AAGCTTACAGCCCTTCGGC	Expression in pET28a of CTX-M-9 and CTX-M-16

[a]Primers used for site-directed mutagenesis show one underlined nucleotide corresponding to the modified codon; primers used for cloning in expression vector show the restriction enzyme recognition site as six-letter underline.

inserts sequenced for verification of the identity of bla_{CTX-M} genes and generated restriction sites, as well as the absence of aberrant nucleotides. Resulting recombinant pTZ57R/T plasmids were then digested, and the released inserts were subsequently purified and cloned in a pET28a(+) vector previously digested with the appropriate restriction enzymes. Ligation mixtures were used to first transform *E. coli* DH5α competent cells. Selected recombinant clones were sequenced for confirming the identity of the bla_{CTX-M} genes, and those harboring the resulting pET plasmids were used for a second transformation step in *E. coli* BL21(DE3) competent cells for protein expression experiments. DNA sequences were determined at Macrogen Inc. (South Korea). Nucleotide and amino acid sequence analyses were conducted by NCBI (http://www.ncbi.nlm.nih.gov/) and ExPASy (http://www.expasy.org/) analysis tools.

***In vitro* susceptibility testing.** MICs of the different β-lactams were obtained by the agar dilution method for recombinant *E. coli* DH5α clones containing plasmids pK12, pK96, pK2, pK131, pK8, pK8Asp240Gly, pK9, pK16, pK78, and pK78Asp240Gly. To evaluate behavior against CAZ and CTX in an isogenic context expressing or not expressing OmpF, MICs for recombinant *E. coli* K-12 and JF703 clones containing all pK_{CTX-M} plasmids were evaluated by microdilution against both antibiotics. Both methods were performed according to the Clinical and Laboratory Standards Institute (CLSI) guidelines. Controls were included, using empty pK19 vector as donor DNA. Positive transformant clones were selected in Luria-Bertani (LB) agar plates supplemented with 30 μg/ml kanamycin and 2 μg/ml CTX, and the presence of the plasmid was verified by plasmid DNA extraction and visualization in 0.8% agarose gels.

Determination of β-lactamase activity. Crude lysates from overnight cultures of *E. coli* DH5α harboring pK_{CTX-M} plasmids were obtained as described before (47). β-Lactamase activity was determined spectrophotometrically by measuring the hydrolysis of 100 μM CEF as the substrate. One unit of β-lactamase activity was defined as the amount of enzyme hydrolyzing 1 nmol substrate per min (in 20 mM phosphate buffer, pH 7.0) at 25°C. The specific activity was defined as the units of β-lactamase per milligram of protein, determined by the Bio-Rad protein assay kit (Bio-Rad, USA).

Assessment of resistant subpopulations under CAZ and CZA selective pressure. Serial 10-fold dilutions of overnight *E. coli* K-12 cultures expressing CTX-M-12 and CTX-M-96 were plated onto Mueller-Hinton agar (MHA) plates containing increasing concentrations of CAZ or CZA (4 mg/liter) to search for the presence of preexisting high-level-resistant mutants. Viable count ($\log_{10}$ CFU/ml) was plotted against antibiotic or antibiotic/inhibitor concentration. *E. coli* K-12 alone and expressing pK19 were used as controls. Antimicrobial susceptibility of the clones tested, as well as 2 intratreatment selected mutants, was confirmed by the microdilution method as described above.

Production and purification of CTX-M β-lactamases. Overnight cultures of recombinant *E. coli* BL21 clones producing CTX-M-12, CTX-M-96, CTX-M-2, CTX-M-131, CTX-M-8, CTX-M-8Asp240Gly, CTX-M-9, CTX-M-16, CTX-M-78, and CTX-M-78Asp240Gly grown in LB broth containing 30 μg/ml kanamycin were diluted 1/20 in 500 ml of the same culture medium and grown at 37°C until an optical density of

0.9 at 600 nm was reached. Isopropyl-β-D-thiogalactopyranoside (IPTG), at a final concentration of 1 mM, was added to induce β-lactamase expression. After 20 h of incubation at 28°C, crude extracts were obtained through ultrasonic disruption, and after clarification by centrifugation at 10,000 × *g* for 30 min (4°C, Sorvall SS34 rotor), clear supernatants containing CTX-M were dialyzed overnight against 2.5 liters of buffer A (50 mM Tris, 200 mM NaCl, pH 8.0). Clear supernatants were filtered by 0.45-μm-pore-size membranes and loaded onto a 5-ml HisTrap HP column (GE Healthcare Life Sciences, USA) connected to an ÄKTA purifier (GE Healthcare Life Sciences, USA) and preequilibrated with buffer A.

The column was extensively washed to remove unbound proteins, and β-lactamases were eluted with a linear gradient (0 to 100%; 2-ml/min flow rate) of buffer B (buffer A plus 500 mM imidazole). Eluted fractions were analyzed by SDS-PAGE in 12% polyacrylamide gels, and β-lactamase activity was assessed in all fractions by nitrocefin hydrolysis. Active fractions were pooled and dialyzed overnight against PBS buffer. Thrombin digestion (GE Healthcare Life Sciences, USA) was performed at 16°C to remove the histidine tag, according to the manufacturer's indications, and removed by affinity chromatography in 1-ml HisTrap HP columns. Eluted proteins were conserved at −70°C until use. Protein concentration and purity were determined by UV absorbance at 280 nm (according to Lambert-Beer law and molar extinction coefficient) and by Coomassie blue staining on 15% SDS-PAGE gels, respectively.

Kinetics. Steady-state kinetic parameters were determined using a T80 UV-visible spectrophotometer (PG Instruments Ltd., UK). Each reaction was performed in a total volume of 500 μl at room temperature (25°C) in 25 mM phosphate buffer, pH 7.0. The steady-state kinetic parameters K_m and V_{max} for CEF and CTX were obtained under initial rates as described previously (31), with nonlinear least-squares fitting of the data (Henri Michaelis-Menten equation) using GraphPad Prism 5.03 for Windows (GraphPad Software, San Diego, CA USA):

$$v = \frac{V_{max} \times [S]}{K_m + [S]} \quad (1)$$

In the case of CAZ, as hydrolysis velocities did not approach saturation at testable concentrations, the slope of the velocity versus antibiotic concentration plot was considered the second-order rate constant for hydrolysis at steady state, k_{cat}/K_m. Inhibition constant K_i was determined by monitoring the residual activity of the enzyme in the presence of various concentrations of CAZ and 100 μM nitrocefin as reporter substrate; the corrected K_i (considered the observed or apparent K_m) value was finally determined using the equation

$$K_i = \frac{K_{i\,obs}}{\left(1 + [S]\right)/K_{m(S)}} K \quad (2)$$

where $K_{m(S)}$ and [*S*] are the reporter substrate's K_m and fixed concentration used, respectively. Due to slight inhibition of nitrocefin hydrolysis even in the presence of high concentrations of CAZ, CTX-M enzymes were preincubated for 1 and 2 h with 0, 100, 200, 400, 580, 1,790, 3,500, and 8,200 μM CAZ prior to the addition of nitrocefin and subsequent measurement of β-lactamase activity. Preincubation with CEF at 50 and 500 μM served as a control in this assay.

The interaction of CTX-M enzymes with AVI was assumed to follow the models of other β-lactamases except KPC-2 (32). Inhibition constants K_i and k_2/K were determined as reported previously (30).

The following extinction coefficients and wavelengths were used (34): CEF ($\Delta\varepsilon_{273}$ of −6,300 M^{-1} cm^{-1}), CAZ ($\Delta\varepsilon_{260}$ of −9,000 M^{-1} cm^{-1}), CTX ($\Delta\varepsilon_{260}$ of −7,500 M^{-1} cm^{-1}), and nitrocefin (λ = 482 nm; $\Delta\varepsilon_{482}$ of +15,000 M^{-1} cm^{-1}).

Circular dichroism. CD spectra were recorded on a Jasco J-810 spectropolarimeter. Data in the near-UV (250 to 320 nm) and far-UV (200 to 250 nm) regions were collected at 25°C using 10- or 1-mm-path-length cuvettes, respectively. A scan speed of 20 nm/min with a time constant of 1 s was used for both proteins. Each spectrum was measured at least three times, and the data were averaged to minimize noise. Molar ellipticity was calculated as described elsewhere (48), using a mean residue weight value of 107.

Fluorescence measurements. Fluorescence measurements were performed at 25°C in a Jasco FP-6500 spectrofluorimeter equipped with a thermostated cell. A 3-mm-path cuvette sealed with a Teflon cap was used. The excitation wavelength was 295 nm, and emission was collected in the range of 300 to 410 nm. The excitation and emission monochromator slit widths were both set at 3 nm.

Thermal denaturation. Thermal unfolding was monitored by the change of the dichroic signal at 222 nm. The dynode voltage (voltage applied to the photomultiplier tube to compensate for the reduction in light intensity) was recorded simultaneously. Each protein sample (200 μl; 8 to 16 μM) contained in a 1-mm cell cuvette was gradually heated from 25 to 60°C at a scan rate of 1°C min^{-1}.

For the spectroscopic techniques, phosphate-buffered saline (137 mM NaCl, 2.7 mM KCl, 1.5 mM KH_2PO_4, 8 mM Na_2HPO_4) was used.

Simulated modeling of CTX-M-96 in complex with AVI. The X-ray structure of CTX-M-96 (PDB entry 3ZNY [24]) previously obtained by our group was used to model the acyl-enzyme structure with AVI. The reference structure, with PDB code 4HBU (CTX-M-15 in complex with AVI [34]), was used for initial positioning of the ligand in the CTX-M-96 structure. Simulation structure was energy minimized with the program Yasara (49), using a standard protocol consisting of a steepest descent minimization followed by simulated annealing of the ligand and protein side chains. CTX-M-96 backbone atoms were kept fixed during the whole procedure. Simulation parameters consisted of the use of AMBER14 force field (50), a cutoff distance of 7.86 Å, particle mesh Ewald (PME) long-range electrostatics (51), periodic boundary conditions, and a water-filled simulation cell.

ACKNOWLEDGMENTS

This work was funded in part by grants from the University of Buenos Aires (UBACyT 2014-2017 to P.P. and 2013-2015 to G.G.) and Agencia Nacional de Promoción Científica y Tecnológica (BID PICT 2015-1925 to G.G. and PICT 2014-0457 to P.P.). Research reported in this publication was supported in part by the National Institute of Allergy and Infectious Diseases of the National Institutes of Health, under award numbers R01AI100560, R01AI063517, R21AI114508, and R01AI072219 to R.A.B. This study was supported in part by funds and/or facilities provided by the Cleveland Department of Veterans Affairs, award number 1I01BX001974 to R.A.B., from the Biomedical Laboratory Research & Development Service of the VA Office of Research and Development, and the Geriatric Research Education and Clinical Center VISN 10 to R.A.B.

The content is solely the responsibility of the authors and does not necessarily represent the official views of the National Institutes of Health or the Department of Veterans Affair.

P.P., B.G., M.M.R., L.C., and G.G. are researchers at the Consejo Nacional de Investigaciones Científicas y Técnicas (CONICET, Argentina).

REFERENCES

1. Gutkind GO, Di Conza J, Power P, Radice M. 2013. β-Lactamase-mediated resistance: a biochemical, epidemiological and genetic overview. Curr Pharm Des 19:164–208. https://doi.org/10.2174/138161213804070320.
2. Rossolini GM, D'Andrea MM, Mugnaioli C. 2008. The spread of CTX-M-type extended-spectrum β-lactamases. Clin Microbiol Infect 14(Suppl 1):S33–S41. https://doi.org/10.1111/j.1469-0691.2007.01867.x.
3. Canton R, Coque TM. 2006. The CTX-M β-lactamase pandemic. Curr Opin Microbiol 9:466–475. https://doi.org/10.1016/j.mib.2006.08.011.
4. Decousser JW, Poirel L, Nordmann P. 2001. Characterization of a chromosomally encoded extended-spectrum class A β-lactamase from *Kluyvera cryocrescens*. Antimicrob Agents Chemother 45:3595–3598. https://doi.org/10.1128/AAC.45.12.3595-3598.2001.
5. Rodriguez MM, Power P, Radice M, Vay C, Famiglietti A, Galleni M, Ayala JA, Gutkind G. 2004. Chromosome-encoded CTX-M-3 from *Kluyvera ascorbata*: a possible origin of plasmid-borne CTX-M-1-derived cefotaximases. Antimicrob Agents Chemother 48:4895–4897. https://doi.org/10.1128/AAC.48.12.4895-4897.2004.
6. Bonnet R. 2004. Growing group of extended-spectrum β-lactamases: the CTX-M enzymes. Antimicrob Agents Chemother 48:1–14. https://doi.org/10.1128/AAC.48.1.1-14.2004.
7. Bradford PA. 2001. Extended-spectrum β-lactamases in the 21st century: characterization, epidemiology, and detection of this important resistance threat. Clin Microbiol Rev 14:933–951. https://doi.org/10.1128/CMR.14.4.933-951.2001.
8. Giani T, Cannatelli A, Di Pilato V, Testa R, Nichols WW, Rossolini GM. 2016. Inhibitory activity of avibactam against selected β-lactamases expressed in an isogenic *Escherichia coli* strain. Diagn Microbiol Infect Dis 86:83–85. https://doi.org/10.1016/j.diagmicrobio.2016.03.002.
9. Lomovskaya O, Sun D, Rubio-Aparicio D, Nelson K, Tsivkovski R, Griffith DC, Dudley MN. 2017. Vaborbactam: spectrum of β-lactamase inhibition and impact of resistance mechanisms on activity in *Enterobacteriaceae*. Antimicrob Agents Chemother 61:e01443-17. https://doi.org/10.1128/AAC.01443-17.
10. Shimizu-Ibuka A, Oishi M, Yamada S, Ishii Y, Mura K, Sakai H, Matsuzawa H. 2011. Roles of residues Cys69, Asn104, Phe160, Gly232, Ser237, and Asp240 in extended-spectrum β-lactamase Toho-1. Antimicrob Agents Chemother 55:284–290. https://doi.org/10.1128/AAC.00098-10.
11. Perez-Llarena FJ, Kerff F, Abian O, Mallo S, Fernandez MC, Galleni M, Sancho J, Bou G. 2011. Distant and new mutations in CTX-M-1 β-lactamase affect cefotaxime hydrolysis. Antimicrob Agents Chemother 55:4361–4368. https://doi.org/10.1128/AAC.00298-11.
12. Novais A, Canton R, Coque TM, Moya A, Baquero F, Galan JC. 2008. Mutational events in cefotaximase extended-spectrum β-lactamases of the CTX-M-1 cluster involved in ceftazidime resistance. Antimicrob Agents Chemother 52:2377–2382. https://doi.org/10.1128/AAC.01658-07.
13. Delmas J, Leyssene D, Dubois D, Birck C, Vazeille E, Robin F, Bonnet R. 2010. Structural insights into substrate recognition and product expulsion in CTX-M enzymes. J Mol Biol 400:108–120. https://doi.org/10.1016/j.jmb.2010.04.062.
14. Adamski CJ, Cardenas AM, Brown NG, Horton LB, Sankaran B, Prasad BV, Gilbert HF, Palzkill T. 2015. Molecular basis for the catalytic specificity of the CTX-M extended-spectrum β-lactamases. Biochemistry 54:447–457. https://doi.org/10.1021/bi501195g.
15. Chen Y, Delmas J, Sirot J, Shoichet B, Bonnet R. 2005. Atomic resolution structures of CTX-M β-lactamases: extended spectrum activities from increased mobility and decreased stability. J Mol Biol 348:349–362. https://doi.org/10.1016/j.jmb.2005.02.010.
16. Cartelle M, del Mar Tomas M, Molina F, Moure R, Villanueva R, Bou G. 2004. High-level resistance to ceftazidime conferred by a novel enzyme, CTX-M-32, derived from CTX-M-1 through a single Asp240-Gly substitution. Antimicrob Agents Chemother 48:2308–2313. https://doi.org/10.1128/AAC.48.6.2308-2313.2004.
17. Bae IK, Lee BH, Hwang HY, Jeong SH, Hong SG, Chang CL, Kwak HS, Kim HJ, Youn H. 2006. A novel ceftazidime-hydrolysing extended-spectrum β-lactamase, CTX-M-54, with a single amino acid substitution at position 167 in the omega loop. J Antimicrob Chemother 58:315–319. https://doi.org/10.1093/jac/dkl252.
18. Bonnet R, Dutour C, Sampaio JL, Chanal C, Sirot D, Labia R, De Champs C, Sirot J. 2001. Novel cefotaximase (CTX-M-16) with increased catalytic efficiency due to substitution Asp-240→Gly. Antimicrob Agents Chemother 45:2269–2275. https://doi.org/10.1128/AAC.45.8.2269-2275.2001.
19. Bonnet R, Recule C, Baraduc R, Chanal C, Sirot D, De Champs C, Sirot J. 2003. Effect of D240G substitution in a novel ESBL CTX-M-27. J Antimicrob Chemother 52:29–35. https://doi.org/10.1093/jac/dkg256.
20. Poirel L, Gniadkowski M, Nordmann P. 2002. Biochemical analysis of the ceftazidime-hydrolysing extended-spectrum β-lactamase CTX-M-15 and of its structurally related β-lactamase CTX-M-3. J Antimicrob Chemother 50:1031–1034. https://doi.org/10.1093/jac/dkf240.
21. Patel MP, Fryszczyn BG, Palzkill T. 2015. Characterization of the global stabilizing substitution A77V and its role in the evolution of CTX-M β-lactamases. Antimicrob Agents Chemother 59:6741–6748. https://doi.org/10.1128/AAC.00618-15.
22. Canton R, Gonzalez-Alba JM, Galan JC. 2012. CTX-M enzymes: origin and diffusion. Front Microbiol 3:110. https://doi.org/10.3389/fmicb.2012.00110.
23. Papp-Wallace KM, Bajaksouzian S, Abdelhamed AM, Foster AN, Winkler ML, Gatta JA, Nichols WW, Testa R, Bonomo RA, Jacobs MR. 2015. Activities of ceftazidime, ceftaroline, and aztreonam alone and combined with avibactam against isogenic *Escherichia coli* strains expressing selected single β-lactamases. Diagn Microbiol Infect Dis 82:65–69. https://doi.org/10.1016/j.diagmicrobio.2015.02.003.
24. Ghiglione B, Rodriguez MM, Herman R, Curto L, Dropa M, Bouillenne F, Kerff F, Galleni M, Charlier P, Gutkind G, Sauvage E, Power P. 2015. Structural and kinetic insights into the "ceftazidimase" behavior of the

extended-spectrum β-lactamase CTX-M-96. Biochemistry 54:5072–5082. https://doi.org/10.1021/acs.biochem.5b00313.
25. Benjwal S, Verma S, Rohm KH, Gursky O. 2006. Monitoring protein aggregation during thermal unfolding in circular dichroism experiments. Protein Sci 15:635–639. https://doi.org/10.1110/ps.051917406.
26. Angelani CR, Caramelo JJ, Curto LM, Delfino JM. 2017. Structural coalescence underlies the aggregation propensity of a beta-barrel protein motif. PLoS One 12:e0170607. https://doi.org/10.1371/journal.pone.0170607.
27. Costa Ramos JM, Stein C, Pfeifer Y, Brandt C, Pletz MW, Makarewicz O. 2015. Mutagenesis of the CTX-M-type ESBL-is MIC-guided treatment according to the new EUCAST recommendations a safe approach? J Antimicrob Chemother 70:2528–2535. https://doi.org/10.1093/jac/dkv153.
28. Winkler ML, Papp-Wallace KM, Taracila MA, Bonomo RA. 2015. Avibactam and inhibitor-resistant SHV β-lactamases. Antimicrob Agents Chemother 59:3700–3709. https://doi.org/10.1128/AAC.04405-14.
29. Papp-Wallace KM, Winkler ML, Gatta JA, Taracila MA, Chilakala S, Xu Y, Johnson JK, Bonomo RA. 2014. Reclaiming the efficacy of β-lactam-β-lactamase inhibitor combinations: avibactam restores the susceptibility of CMY-2-producing *Escherichia coli* to ceftazidime. Antimicrob Agents Chemother 58:4290–4297. https://doi.org/10.1128/AAC.02625-14.
30. Ruggiero M, Papp-Wallace KM, Taracila MA, Mojica MF, Bethel CR, Rudin SD, Zeiser ET, Gutkind G, Bonomo RA, Power P. 2017. Exploring the landscape of diazabicyclooctane (DBO) inhibition: avibactam (AVI) inactivation of PER-2 β-lactamase. Antimicrob Agents Chemother 61:e02476-16. https://doi.org/10.1128/AAC.02476-16.
31. Ehmann DE, Jahic H, Ross PL, Gu RF, Hu J, Durand-Reville TF, Lahiri S, Thresher J, Livchak S, Gao N, Palmer T, Walkup GK, Fisher SL. 2013. Kinetics of avibactam inhibition against class A, C, and D β-lactamases. J Biol Chem 288:27960–27971. https://doi.org/10.1074/jbc.M113.485979.
32. Ehmann DE, Jahic H, Ross PL, Gu RF, Hu J, Kern G, Walkup GK, Fisher SL. 2012. Avibactam is a covalent, reversible, non-β-lactam β-lactamase inhibitor. Proc Natl Acad Sci U S A 109:11663–11668. https://doi.org/10.1073/pnas.1205073109.
33. Krishnan NP, Nguyen NQ, Papp-Wallace KM, Bonomo RA, van den Akker F. 2015. Inhibition of *Klebsiella* β-lactamases (SHV-1 and KPC-2) by avibactam: a structural study. PLoS One 10:e0136813. https://doi.org/10.1371/journal.pone.0136813.
34. Lahiri SD, Mangani S, Durand-Reville T, Benvenuti M, De Luca F, Sanyal G, Docquier JD. 2013. Structural insight into potent broad-spectrum inhibition with reversible recyclization mechanism: avibactam in complex with CTX-M-15 and *Pseudomonas aeruginosa* AmpC β-lactamases. Antimicrob Agents Chemother 57:2496–2505. https://doi.org/10.1128/AAC.02247-12.
35. Kang CI, Cha MK, Kim SH, Wi YM, Chung DR, Peck KR, Lee NY, Song JH. 2014. Extended-spectrum cephalosporins and the inoculum effect in tests with CTX-M-type extended-spectrum β-lactamase-producing *Escherichia coli*: potential clinical implications of the revised CLSI interpretive criteria. Int J Antimicrob Agents 43:456–459. https://doi.org/10.1016/j.ijantimicag.2014.01.030.
36. Bush K. 2015. A resurgence of β-lactamase inhibitor combinations effective against multidrug-resistant Gram-negative pathogens. Int J Antimicrob Agents 46:483–493. https://doi.org/10.1016/j.ijantimicag.2015.08.011.
37. Shen Z, Ding B, Bi Y, Wu S, Xu S, Xu X, Guo Q, Wang M. 2016. CTX-M-190, a novel β-lactamase resistant to tazobactam and sulbactam, identified in an *Escherichia coli* clinical isolate. Antimicrob Agents Chemother 61:e01848-16.
38. Cai J, Cheng Q, Shen Y, Gu D, Fang Y, Chan EW, Chen S. 2017. Genetic and functional characterization of $bla_{ctx\text{-}m\text{-}199}$, a novel tazobactam and sulbactam resistance-encoding gene located in a conjugative mcr-1-bearing IncI2 plasmid. Antimicrob Agents Chemother 61:e00562-17. https://doi.org/10.1128/AAC.00562-17.
39. Novais A, Comas I, Baquero F, Canton R, Coque TM, Moya A, Gonzalez-Candelas F, Galan JC. 2010. Evolutionary trajectories of β-lactamase CTX-M-1 cluster enzymes: predicting antibiotic resistance. PLoS Pathog 6:e1000735. https://doi.org/10.1371/journal.ppat.1000735.
40. Bush K, Bradford PA. 2016. β-Lactams and β-lactamase inhibitors: an overview. Cold Spring Harb Perspect Med 6:a025247. https://doi.org/10.1101/cshperspect.a025247.
41. Livermore DM, Mushtaq S, Nguyen T, Warner M. 2011. Strategies to overcome extended-spectrum β-lactamases (ESBLs) and AmpC β-lactamases in shigellae. Int J Antimicrob Agents 37:405–409. https://doi.org/10.1016/j.ijantimicag.2010.11.028.
42. Ripoll A, Baquero F, Novais A, Rodriguez-Dominguez MJ, Turrientes MC, Canton R, Galan JC. 2011. In vitro selection of β-lactam plus β-lactamase inhibitor resistant variants in CTX-M β-lactamases: predicting the in-vivo scenario? Antimicrob Agents Chemother 55:4530–4536. https://doi.org/10.1128/AAC.00178-11.
43. Livermore DM, Andrews JM, Hawkey PM, Ho PL, Keness Y, Doi Y, Paterson D, Woodford N. 2012. Are susceptibility tests enough, or should laboratories still seek ESBLs and carbapenemases directly? J Antimicrob Chemother 67:1569–1577. https://doi.org/10.1093/jac/dks088.
44. Clinical and Laboratory Standards Institute. 2013. Performance standards for antimicrobial susceptibility testing; twenty-third informational supplement M100-S22, vol 33. Clinical and Laboratory Standards Institute, Wayne, PA.
45. Foulds J, Chai T. 1979. Isolation and characterization of isogenic *E. coli* strains with alterations in the level of one or more major outer membrane proteins. Can J Microbiol 25:423–427. https://doi.org/10.1139/m79-065.
46. Pridmore RD. 1987. New and versatile cloning vectors with kanamycin-resistance marker. Gene 56:309–312. https://doi.org/10.1016/0378-1119(87)90149-1.
47. Power P, Radice M, Barberis C, de Mier C, Mollerach M, Maltagliatti M, Vay C, Famiglietti A, Gutkind G. 1999. Cefotaxime-hydrolysing β-lactamases in *Morganella morganii*. Eur J Clin Microbiol Infect Dis 18:743–747. https://doi.org/10.1007/s100960050391.
48. Schmid F. 1989. Spectral methods of characterizing protein conformation and conformational changes. *In* Creighton TE (ed), Protein structure: a practical approach. IRL, New York, NY.
49. Krieger E, Darden T, Nabuurs SB, Finkelstein A, Vriend G. 2004. Making optimal use of empirical energy functions: force-field parameterization in crystal space. Proteins 57:678–683. https://doi.org/10.1002/prot.20251.
50. Krieger E, Joo K, Lee J, Raman S, Thompson J, Tyka M, Baker D, Karplus K. 2009. Improving physical realism, stereochemistry, and side-chain accuracy in homology modeling: four approaches that performed well in CASP8. Proteins 77:114–122. https://doi.org/10.1002/prot.22570.
51. Essmann U, Perera L, Berkowitz ML, Darden T, Lee H, Pedersen LG. 1995. A smooth particle mesh Ewald method. J Chem Phys 103:8577–8593. https://doi.org/10.1063/1.470117.